

Effect of surfactant treated boehmite nanoparticles on properties of block copolymers

R. Adhikari¹, W. Brostow^{*2}, T. Datashvili², S. Henning³, B. Menard², K. P. Menard^{2,4} and G. H. Michler⁵

The effectiveness of reinforcement of a polymer is known to depend on the strength of the interfaces between the reinforcement and the matrix. We have used polystyrene and a styrene–butadiene–styrene (SBS) copolymer as matrixes and ceramic boehmite γ -AlO(OH) as reinforcement. We have applied boehmite both untreated and treated with sulphonic acid based surfactants with different alkyl groups. As expected, the coupling agents improve the adhesion between the polymers and the ceramic filler. The presence of boehmite and treatments affect the glass transition temperatures determined by dynamic mechanical analysis, nanoindentation hardness $h_{\text{nanoindent}}$ as well as Vickers microhardness h_{Vickers} . For SBS and SBS containing composites, the $h_{\text{nanoindent}}/h_{\text{Vickers}}$ ratio is a constant.

Keywords: Polymer reinforcement, Boehmite, Surface modification, Polystyrene, Styrene/butadiene/styrene, Vickers hardness, Nanoindentation hardness

Introduction

There is a large variety of polymer based materials. Some of them are created for the improvement of electrical, tribological or acoustic properties, but the majority is developed to achieve better mechanical properties.^{1–3} Among the classes of polymer based materials, we have block copolymers in which the constituents are microphase separated into ordered nanostructures.⁴ This allows a fairly wide range of properties that can be varied.

A composite material is made out of two or more parts, each of which gives certain properties. Wood is a natural composite, which has fibres that provide strength and are held together by a matrix.⁵ The aerospace industry uses many composites in aeroplanes, such as the American F-22, where carbon fibres are embedded in an epoxy matrix.⁶

Most composites currently made are macro- or microcomposites. In fibre reinforced ones, the fibres have strong effects on certain properties but less effect on some other properties. For example, if the glass transition temperature T_g of an epoxy is measured with

and without fibres in it, the transition temperature of the epoxy resin does not change.⁷

Recently, nanocomposites are being made containing particles with diameters measured in nanometres.⁸ Such materials can also be used, for instance, in food packaging since they produce a good barrier to gases, which allows longer storage times. Other avenues of research in nanocomposites are electrical and thermal conductivities and body armour for soldiers and police. In the present work, how a series of modified nanoparticles affect certain properties of thermoplastics was investigated.

T_g is known to be an indicator for changes in material properties.^{9–11} It actually represents a region in which the transition takes place; for convenience, a single number is used. We decided to track the T_g values of a series of materials made with nanoparticles of boehmite, an aluminium oxide hydroxide [γ -AlO(OH)] mineral. These nanoparticles were used both untreated and treated with sulphonic acid based surfactants with different alkyl groups. As matrixes, polystyrene–polybutadiene–polystyrene (SBS) triblock copolymers were used. They behave as cross-linked elastomers at ambient conditions and are processable at elevated temperatures, while their properties can be tuned by changing the composition of the constituents and their molecular architectures.¹² For comparison, the corresponding nanocomposites of polystyrene (PS) homopolymer were also investigated.

The best way to measure T_g is by dynamic mechanical analysis (DMA) due to the high sensitivity of this technique.^{9–11} The microindentation measurements were also performed as representative for the tribology of the material and Vickers hardness was determined.

¹Central Department of Chemistry, Tribhuvan University, Kathmandu, Nepal

²Laboratory of Advanced Polymers and Optimized Materials (LAPOM), Department of Materials Science and Engineering and Center for Advanced Research and Technology (CART), University of North Texas, 3940 North Elm Street, Denton, TX 76207, USA

³Fraunhofer Institute for Materials Mechanics, Walter-Hülse-Strasse 1, Halle 06120, Germany

⁴PerkinElmer LSAS, 761 Bridgeport Avenue, MS71, Shelton, CT 06484, USA

⁵Institute of Physics and Institute of Polymeric Materials, Martin Luther University of Halle–Wittenberg, Halle–Wittenberg, Germany

*Corresponding author, email wbrostow@yahoo.com

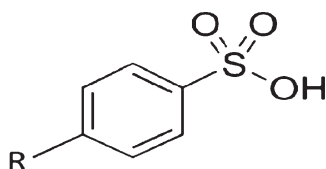
Experimental

Materials

The PS sample is a commercial product of BASF SE, Ludwigshafen, Germany, under the trade name of PS 158k, and has a number average molecular weight of $8.20 \times 10^4 \text{ g mol}^{-1}$ and a polydispersity index $M_w/M_n=2.30$, where M_w is the weight average molecular mass, while M_n is the number average molecular mass. The SBS copolymer, to be called below ST3, is a star block copolymer also supplied by BASF SE. It contains 74 wt-%PS and 26 wt-% polybutadiene and has M_n of $8.57 \times 10^4 \text{ g mol}^{-1}$, whereby the polydispersity index is 2.10. The sample was synthesised by butyl lithium initiated anionic polymerisation; more details of the synthesis have been provided in Ref. 12.

The boehmite nanofillers were supplied by Sasol Chemical Co. The characteristics of the fillers used are presented in Table 1.

The general chemical structure of the surfactants used can be represented as



where R is either the $-\text{CH}_3$ group or a mixture of C_{10} to C_{13} straight chain alkyl groups for the sulphonic acids. Undecanoic acid is a simple straight chained carboxylic acid.

The components were mixed in a Brabender mixer for 5 min and compression moulded at the pressure of 120 bar at 200°C for 5 min. This part of work was performed in Halle. Table 2 gives the composition of the samples produced.

Specimens for testing were prepared at North Texas from the samples made in Halle. Samples were cut into multiple strips and then measured with a micrometer to two decimal places in length, width and thickness.

Electron microscopy analysis of samples

The block copolymer and some of the blends and nanocomposites were investigated by transmission electron microscopy (TEM) and scanning electron microscopy (SEM). For the TEM analyses, the specimens were prepared by ultramicrotomy of each sample followed by staining with osmium tetroxide vapour so that the double bond containing butadiene phase appears darker in the TEM images. The ultrathin sections were investigated by a 120 kV LEO 912 TEM. For the SEM analyses of the samples, each sample was cryofractured using liquid nitrogen, and the fracture surface was coated with a thin film of carbon. The specimens were investigated by means of a JEOL JSM

Table 2 Compositions of materials

Base polymer	Filler type and weight content
ST3	...
ST3	5 wt-%OS1
ST3	5 wt-%OS2
ST3	5 wt-%HP14
PS	...
ST3/PS (80:20)	...
ST3/PS (80:20)	5 wt-%OS1
ST3+PS (80:20 by weight)	5 wt-%OS2
ST3+PS (80:20 by weight)	5 wt-%HP14

6300 SEM in backscattered electron (BSE) imaging mode.

Dynamic mechanical analysis

The samples were loaded into a PerkinElmer DMA 8000 machine with a single cantilever fixture. The technique has been described by one of us.⁹⁻¹¹ The materials were studied over temperatures ranging from -125 to $+150^\circ\text{C}$. The DMA was cooled using liquid nitrogen. The samples were run at three frequencies of 0.1, 1.0 and 10.0 Hz and with 0.050 mm of applied strain. The temperature of transitions was calculated following the procedures of the ASTM discussed by Seyler.¹³

Nanoindentation hardness and Vickers hardness

The indentation is made on the surface, creating a unique load–depth curve for the specific sample. Using the tangential slope of the curve and the indenter tip geometry, the software calculates the indentation hardness. The indents may be visually inspected using an integrated, synchronised optical microscope. A TTX-NHT S/N:50-00155 from CSM Instruments, Neuchatel, Switzerland, fitted with a diamond Berkovich indenter (B-K59), with an approach speed of 5000 nm min^{-1} and a delta slope contact of 25%, was used. Data were collected at 10.0 Hz with linear loading and an unloading rate of 100 mN min^{-1} to a maximum of 50 mN. A pause of 6 s between cycles was used.

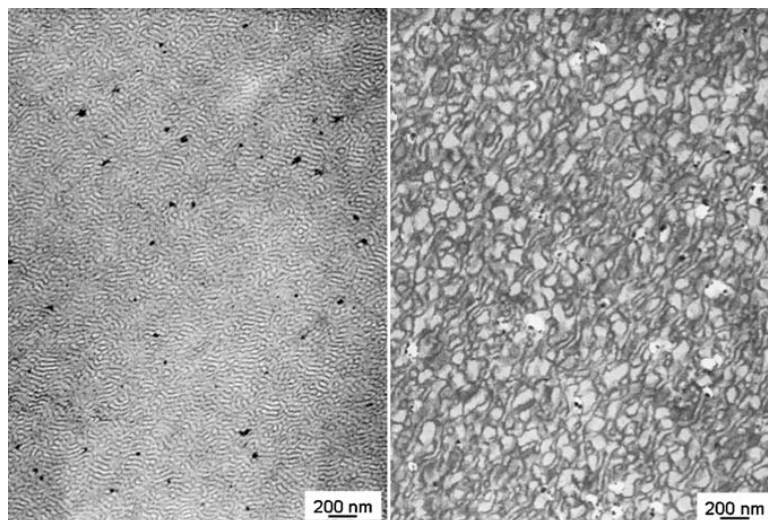
Vickers microhardness h_{Vickers} was determined using a dynamic microhardness measurement device, HMV-M Shimadzu microhardness tester model M3 from Shimadzu Co., Kyoto, Japan. Microindentations were made using a 300 g load. The holding time after completion of the indentation was 5 s. Five indentations were made for each sample. Each mean value of the Vickers microhardness was calculated from five tests using the formula

$$h_{\text{Vickers}} = 1854.4P/d^2 \quad (1)$$

where P is the load in grams, while d is the mean diagonal of the indentation in micrometres. While the resulting value has dimensions, it is customary to list the Vickers microhardness as if it were a dimensionless quantity.^{14,15}

Table 1 Characteristics of nanofillers used in this study

Properties/filler	Disperal OS1	Disperal OS2	Disperal HP14
Surface treatment	<i>p</i> -Toluenesulphonic acid	Alkylbenzenesulphonic acid	Undecanoic acid
Average crystal size/nm	10	10	...
Particles shape	Spherical	Spherical	Needle-like



1 Images (TEM) of pure star block copolymer (left) and ST3/PS (80/20) blend (right); osmium tetroxide staining renders butadiene rich phase which appears dark in images

Electron microscopy results for unindented samples

Figure 1 shows a typical nanostructured morphology of the block copolymer (ST3) and ST3/PS (80/20) blend. The pure block copolymer shows a bicontinuous network of glassy PS phase and rubbery butadiene rich phase. The addition of 20 wt-%PS leads to the formation of droplets of PS embedded in a soft block copolymer matrix, as reported before by some of us.¹⁶

Nanocomposite materials based on the pure block copolymer (ST3) and those based on ST3+PS blends show a similar distribution of the filler particles in the polymeric matrix. As an example, Fig. 2 shows the SEM images of the ST3/PS (80/20) blend comprising 5 wt-% of OS1 nanofiller (Fig. 2a), OS2 (Fig. 2b) and HP14 (Fig. 2c). As mentioned above, the BSE mode was used. In general, higher atomic numbers of the atoms result in higher efficiency of BSE emission, leading to a brighter contrast in the micrographs. Thus, in our case, the brighter regions in the micrographs represent the inorganic fillers rather than the low atomic mass elements present in the organic polymer.

An inspection of the SEM images of the samples easily reveals that the blend containing HP13 as a filler contains large filler aggregates, whereas the blend comprising O1 exhibits smaller inorganic particles. The

blend with OS2 shows no clear appearance of the filler; it can be inferred that we are dealing here with uniform distribution of the filler without aggregation.

Dynamic mechanical analysis results

In DMA experiments, a sinusoidal stress σ is applied as a function of time t

$$\sigma t = \sigma_0 \sin(2\pi\nu t) \quad (2)$$

where ν is the frequency in hertz. The result of imposition of the sinusoidal load results in the following behaviour of the strain ε

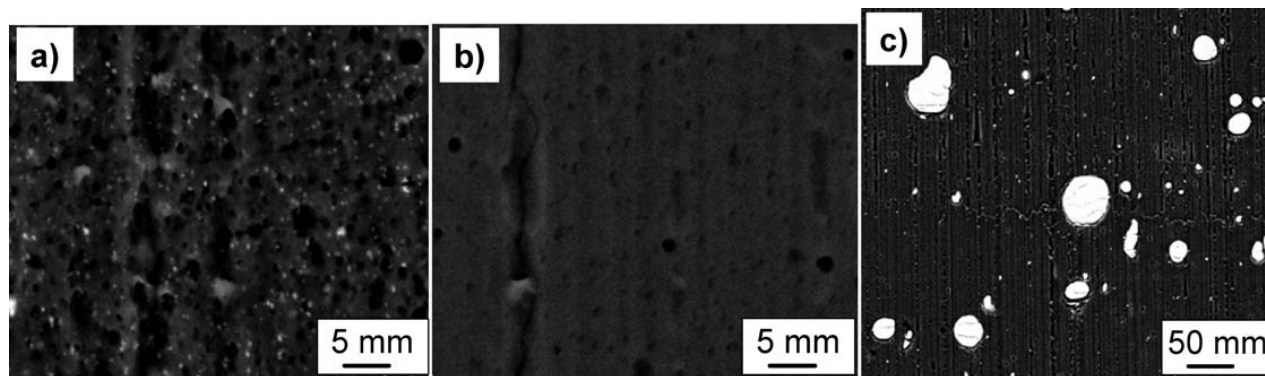
$$\varepsilon t = \varepsilon_0 \sin(2\pi\nu t - \delta) \quad (3)$$

If the material is fully elastic, then we have $\delta=0$. In a viscoelastic material, there always is a phase lag between stress and strain so that $\delta \neq 0$.

For a given deformation mode (such as the cantilever used by us), we have

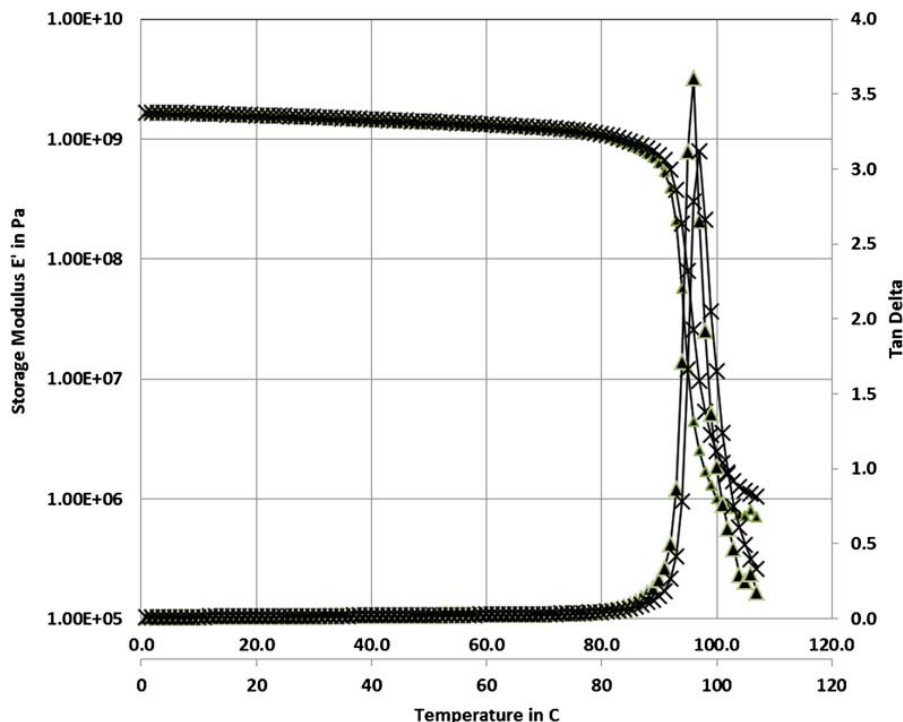
$$\sigma/\varepsilon_0 = E^* = E' + iE'' \quad (4)$$

where E^* is the complex modulus, $i=(-1)^{1/2}$, E' is the storage modulus, which is a measure of the solid-like (elastic) response of the material and E'' is called the loss modulus and corresponds to the liquid-like (viscous flow) response of the material. Since E'' represents



a ST3/PS (80/20)+20%OS1; b ST3/PS (80/20)+20%OS2; c ST3/PS (80/20)+20%HP14

2 Images (SEM) of composites based on block copolymer/PS blends



3 Dynamic mechanical analysis results for PS: only two frequencies are shown for clarity [0.1 Hz (Δ) and 1.0 Hz (X)]. Note shift in major drop in E' and in peak of $\tan \delta$ with increased frequency. On left, curves at top which then descend at higher temperatures are those for E' ; curves which, on left, are close to bottom but then form peaks at higher temperatures are for $\tan \delta$

energy dissipation, it is also a measure of the energy converted to heat. Namely, the heat H created is given by

$$H = \pi E'' \epsilon_0^2 \tag{5}$$

The phase lag δ between stress and strain can be connected to the quantities featured in equation (4), namely

$$\tan \delta = E''/E' \tag{6}$$

An example of the results so obtained is shown in Fig. 3. On the basis of the descents of E' and of peaks of $\tan \delta$, T_g values were obtained, which, for the frequency of 1.0 Hz, are summarised in Table 3.

It is noted that the brittleness B of materials is inversely proportional to the value of storage modulus E' at 1.0 Hz^{17,18} and also that PS is much more brittle than most polymers.¹⁷

As seen in Fig. 3, at the higher frequency of 1.0 Hz, the glass transition shifts to a higher temperature. In general, materials resist deformation. At a lower frequency, a material has more time to adapt to a stress

Table 3 Glass transition temperatures from DMA results

Materials	T_g
ST3	106.5
ST3+5%OS1	108.0
ST3+5%OS2	110.2
ST3+5%HP14	109.1
Pure PS	128.5
ST3+20%PS	111.3
ST3+20%PS+5%OS1	114.1
ST3+20%PS+5%OS2	111.7
ST3+20%PS+5%HP14	111.9

wave defined by equation (2). At a higher frequency, there is less time for adaptation; hence, the material shows more resistance to the force applied. Since above T_g there is more adaptability to deformation, at a higher frequency ν , we have T_g shifting to a higher value.

Consider the results for ST3 reinforced in turn with OS1, OS2 and HP14. The addition of 5 wt-%OS1 increases T_g by 1.5°C. The addition of the same concentration of OS2 increases T_g by 3.7°C, more than a double effect. The addition of HP14 produces a shift by 2.6°C. We recall the order of uniformity of the filler distribution in the matrix found by SEM: the best for OS2, intermediate for HP14 and the worst for OS1. Thus, a more uniform filler distribution results in more 'cooperation' of the filler with the matrix and larger ΔT_g effects.

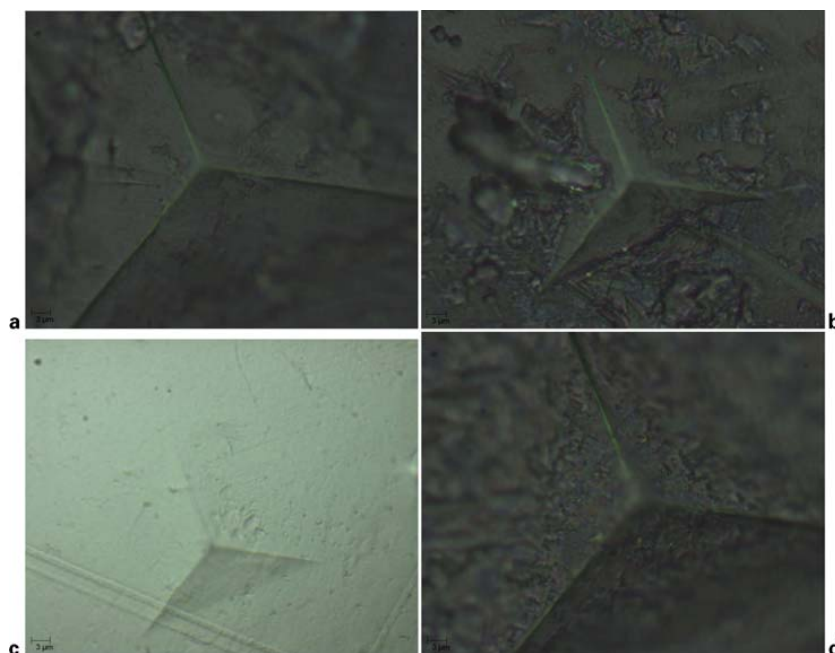
Now, consider pure polymers and the blend of ST3 and PS containing 20 wt-% of the latter. Clearly, T_g value for the blend is much closer to that of pure ST3 than to that of PS. Thus, the presence of PS does not have much effect on the glass transition temperature.

In turn, consider ternary systems formed so that to the ST3+PS blend in the weight proportion 80:20, different forms of boehmite have been added, each time for 5 wt-%. Thus, the value to be used in comparisons is $T_g=111.3^\circ\text{C}$ for the unreinforced blend. Here, OS1 affects the T_g more than OS2. One possible explanation is the strong interaction of OS2 with PS.

Table 4 Indentation and Vickers hardness

Property	ST3	ST3+HP14	ST3+OS1	ST3+OS2
Indentation hardness/MPa	18.4	31.1	129.3	17.6
Vickers hardness	1.70	2.88	11.97	1.62

COLOUR FIGURE



a ST3; b ST3+5%HP14; c ST3+5% OS1; d ST3+5% OS2

4 Images (SEM) of indented surfaces of some of investigated samples

Finally, consider ST3 and PS with 5%HP14 added. Here, the effect of the additive amounts to $\Delta T_g = +2.6^\circ\text{C}$ for the former and $\Delta T_g = -16.6^\circ\text{C}$ for the latter. In other words, boehmite HP14 acts as a reinforcement for the copolymer but as a plasticiser for PS. Given that for PS, we have the very high value $10^{10}B/[\% \text{ Pa}] = 8.78$,¹⁷ this effect is not surprising. We recall the results for low density polyethylene (LDPE) reinforced with boehmite.¹⁹ Low density polyethylene has $10^{10}B/[\% \text{ Pa}] = 0.132$.¹⁷ Static and dynamic friction values of LDPE are lowered by the presence of boehmite, an effect explained by the lubricating action of $-\text{OH}$ groups of boehmite on the LDPE surface.¹⁹ Grafting of coupling agents on the surface of boehmite enhances the friction lowering effect; Kopczyńska and Ehrenstein²⁰ stress the importance of interfaces for properties of multiphase materials. In the same LDPE + boehmite system in the molten state, lowering of viscosity with the addition of boehmite is found,²¹ against the general tendency of solid ceramic additives of increasing viscosity. This unusual effect is caused also by the application of coupling agents, which cause attachment of polymer fibrils to boehmite particles. As a result of good adhesion between the polymer matrix and the mineral filler, the polymer melt with filler flows more uniformly, thus exhibiting a lower viscosity despite adding the solid filler. Thus, a fairly coherent image of the effects of boehmite on the behaviour of polymers seems to emerge.

Nanoindentation and Vickers hardness results

In instrumented indentation testing, an indenter tip normal to the sample surface is driven into the sample by applying an increasing load up to some preset value. The load is then gradually released until partial or complete relaxation of the material occurs. During both loading and unloading cycles, the applied force and penetration depth into the material are recorded, and a

load–displacement curve is created. Using the features of this curve, such as slope, and testing parameters, such as contact area of the tip, the nanoindentation hardness can be determined. Namely, the local hardness $h_{\text{nanoindent}}$ can be calculated as²²

$$h_{\text{nanoindent}} = P/A \quad (7)$$

where P is the load applied to the test surface, and A is the projected contact area at that load. If the materials were fully elastic^{22–24} (which viscoelastic materials never are by definition), Young's modulus could also be calculated. Surprisingly, the method developed by Doerner and Nix²² is often referred to in the literature as 'the Oliver and Pharr method' in spite of the fact that Oliver and Pharr papers on the subject appeared several years later^{23,24} than the original paper by Doerner and Nix.

As described in the section on 'Dynamic mechanical analysis', Vickers microhardness numbers have also been determined. In this method, the values obtained are independent of the size of the indenter. The results obtained are presented in Table 4.

Interestingly, the OS1 filler, which is the most aggregated, provides a much stronger resistance to the indenter than the other fillers, which are distributed more uniformly in the matrix. This applies to both the indentation and the Vickers hardness. Again, the SEM results are useful for understanding these results.

One would expect that the two kinds of hardness could be related, as already suggested in Ref. 15. On the basis of the above results, a simple proportionality has been assumed

$$h_{\text{nanoindent}} = c_h h_{\text{Vickers}} \quad (8)$$

Calculations from the data in Table 2 for the series based on the ST3 copolymer with various reinforcements or without a reinforcement give us the numerical value $c_h = 10.82$. The subscript h stands for hardness. The average deviation from that number is only 0.025.

COLOUR
FIGURE

We recall that the Vickers hardness has also been related by an equation to the total groove area in scratch resistance testing.²⁵ The total groove area consists of the internal area (deeper than the surface) and the external area of two top ridges along the groove (above the surface).

Morphology of indented surfaces

Figure 4 shows some of the SEM images of indented surfaces of several samples. The samples were prepared by sputter coating the specimens with thin films of gold after completion of the indentation tests.

It is apparent that the surface of the composite containing the unmodified boehmite is considerably more textured than those of composites with modified boehmite. This supports our earlier conclusion that the coupling agents improve the adhesion of the polymers to boehmite.

A wide variety of nanocomposites has been investigated before.^{26–40} As already noted, the fact that our SBS block copolymer exhibits microphase separated morphologies⁴⁰ provides additional maneuverability of properties.

References

1. L. E. Nielsen and R. F. Landel: 'Mechanical properties of polymers and composites', 2nd edn; 1994, New York, Marcel Dekker.
2. M. S. Rabello: 'Adivituação de polimeros'; 2000, São Paulo, Artliber.
3. E. Pisanova and S. Zhandarov: in 'Performance of plastics', (ed. W. Brostow), Chap. 19; 2000, Munich/Cincinnati, OH, Hanser.
4. R. Stadler, C. Auschra, J. Beckmann, U. Krappe, I. Voigt-Martin and L. Leibler: *Macromolecules*, 1995, **31**, 3080.
5. W. Brostow, T. Datashvili and H. Miller: *J. Mater. Educ.*, 2010, **32**, 125.
6. W. Goertzen and M. Kessler: *Composites B*, 2007, **38B**, 1.
7. G. Curran, J. Rogers, H. O'Neal, S. Welch and K. P. Menard: *J. Adv. Mater.*, 1995, **26**, 49.
8. S. N. Bhattacharya, M. R. Kamal and R. K. Gupta: 'Polymeric nanocomposites: theory and practice', 317; 2008, Cincinnati, OH, Hanser Gardner.
9. K. P. Menard: in 'Performance of plastics', (ed. W. Brostow), Chap. 8; 2000, Munich/Cincinnati, OH, Hanser.
10. K. P. Menard and B. Bilyeu: 'Dynamic mechanical analysis of polymers and rubbers', in 'Encyclopedia of analytical chemistry online', (ed. F. Rose), 2008, New York, Wiley.
11. K. P. Menard: 'Dynamic mechanical analysis: a practical introduction', 2nd edn, 103; 2008, Boca Raton, FL, CRC Press.
12. R. Adhikari and G. H. Michler: *Prog. Polym. Sci.*, 2004, **29**, 949–986.
13. R. Seyler: in 'Assignment of the glass transition', (ed. R. Seyler), STP 1249, 16; 1994, West Conshohocken, PA, ASTM.
14. W. Brostow, T. Datashvili and B. Huang: *Polym. Eng. Sci.*, 2008, **48**, 292.
15. W. Brostow, T. Datashvili, R. McCarty and J. White: *Mater. Chem. Phys.*, 2010, **124**, 371.
16. R. Adhikari, M. Buschnakowski, W. Lebek, R. Godehardt, G. H. Michler, F. J. Balta Calleja and K. Knoll: *Polym. Adv. Technol.*, 2005, **16**, 175.
17. W. Brostow, H. E. Hagg Lobland and M. Narkis: *J. Mater. Res.*, 2006, **21**, 2422.
18. W. Brostow, H. E. Hagg Lobland and M. Narkis: *Polym. Bull.*, to be published.
19. W. Brostow, T. Datashvili, D. Kao and J. Too: *Polym. Compos.*, 2010, **31**, 417.
20. A. Kopczyńska and G. W. Ehrenstein: *J. Mater. Educ.*, 2007, **29**, 325.
21. P. Blaszcak, W. Brostow, T. Datashvili and H. E. Hagg Lobland: *Polym. Compos.*, 2010, **31**, 1909.
22. M. F. Doerner and W. D. Nix: *J. Mater. Res.*, 1986, **1**, 601.
23. W. C. Oliver and G. M. Pharr: *J. Mater. Res.*, 1992, **7**, 1564.
24. W. C. Oliver and G. M. Pharr: *J. Mater. Res.*, 2004, **19**, 3.
25. W. Brostow, W. Chonkaew, L. Rapoport, Y. Soifer and A. Verdyan: *J. Mater. Res.*, 2007, **22**, 2483.
26. D. S. dos Santos, Jr, P. J. G. Goulet, N. P. W. Pieczonka, O. N. Oliveira, Jr and J. R. Aroca: *Langmuir*, 2004, **20**, 10273–10277.
27. A. Nogales, G. Broza, Z. Roslaniec, K. Schulte, I. Sics, B. S. Hsiao, A. Sanz, M. C. Garcia Gutierrez, D. R. Rueda, C. Domingo and T. A. Ezquerra: *Macromolecules*, 2004, **37**, 7669.
28. K. G. Gatos, R. Thomann and J. Karger-Kocsis: *Polym. Int.*, 2004, **53**, 1191–1197.
29. W. Brostow, M. Keselman, I. Mironi-Harpaz, M. Narkis and R. Peirce: *Polymer*, 2005, **46**, 5058.
30. A. K. Kota, B. H. Cipriano, D. Powell, S. R. Raghavan and H. A. Bruck: *Nanotechnology*, 2007, **18**, 505705.
31. A. Pegoretti, A. Dorigato and A. Penati: *Exp. Polym. Lett.*, 2007, **1**, 123–131.
32. L. F. Giraldo, W. Brostow, E. Devaux, B. L. Lopez and L. D. Perez: *J. Nanosci. Nanotechnol.*, 2008, **8**, 3176.
33. G. Broza and K. Schulte: *Polym. Eng. Sci.*, 2008, **48**, 2033.
34. W. Brostow, W. Chonkaew, T. Datashvili and K. P. Menard: *J. Nanosci. Nanotechnol.*, 2009, **9**, 1916.
35. E. Viguera-Santiago, S. Hernandez-Lopez, W. Brostow, O. Olea-Mejia and O. Lara-Sanjuan: *e-Polymers*, 2010, (100).
36. M.-D. Bermudez, W. Brostow, F. J. Carrion-Vilches and J. Sanes: *J. Nanosci. Nanotechnol.*, 2010, **10**, 6683.
37. O. Olea-Mejia, W. Brostow and E. Buchman: *J. Nanosci. Nanotechnol.*, 2010, **10**, 8524.
38. W. Brostow, M. Dutta, P. Rusek, J. R. de Souza, A. M. de Medeiros and E. N. Ito: *Exp. Polym. Lett.*, 2010, **4**, 570.
39. W. Chonkaew, W. Minghvanish, U. Kunglian, N. Rochanawipart and W. Brostow: *J. Nanosci. Nanotechnol.*, 2011, **11**, 2018.
40. G. H. Michler, R. Adhikari, W. Lebel, S. Goerlitz, R. Weidisch and K. Knoll: *J. Appl. Polym. Sci.*, 2002, **85**, 683.